Meson-meson scattering in EFT's and new exotic hadrons

Raquel Molina

M. Döring, A. Alexandru, D. Guo, B. Hu (GWU)
E. Oset, N. Ikeno (UV), J. Ruiz de Elvira (ITP)

January 26, 2021

Content (PRL105,PRD82(2010),PRD98(2018),JHEP2011(2020), PLB811(2020), 2011.13425 (PLB,2020))

Hadrons

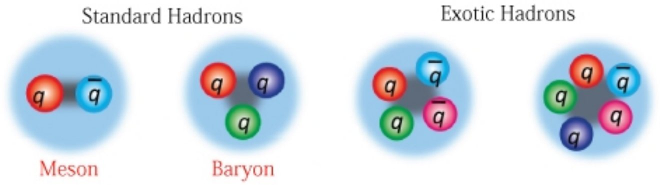

- ’Regular’ hadrons: $q\bar{q}$, qqq

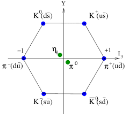

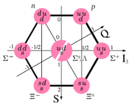

- Exotics: $q\bar{q}q\bar{q}$, $qqqq\bar{q}$, $q\bar{q}g$,...
  Not $q\bar{q}$: $J^{PC} = 0^{+-}, 1^{-+}, 2^{+-}, 3^{-+}$,...

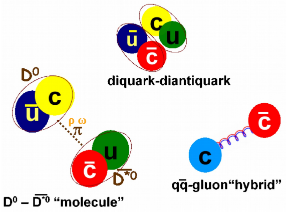

Light hadrons

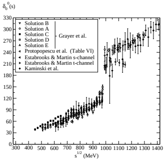

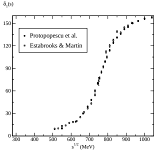

Close to ...

- $\longrightarrow$ PP th. $\pi\pi$, $K\bar{K}$... PB $K\Lambda$, $\pi\Sigma$, $\bar{K}N$...
- $\longrightarrow$ PV th. $K\bar{K}^*$, $\pi\rho$, $\pi\omega$, $\eta\omega$... SB σN...
- $\longrightarrow$ VV th. $\rho\rho$, $K^*\bar{K}^*$... VB $\rho(\omega)N$, K^*N...
- $\longrightarrow$ Hybrid, Glueball candidate

Particle	J^P	overall
N	$1/2^+$	****
$N(1440)$	$1/2^+$	****
$N(1520)$	$3/2^-$	****
$N(1535)$	$1/2^-$	****
$N(1650)$	$1/2^-$	****
$N(1675)$	$5/2^-$	****
$N(1680)$	$5/2^+$	****
$N(1700)$	$3/2^-$	***
$N(1710)$	$1/2^+$	****
$N(1720)$	$3/2^+$	****
$N(1860)$	$5/2^+$	**
$N(1875)$	$3/2^-$	***
$N(1880)$	$1/2^+$	***

			Status as seen in —		
Particle	J^P	Overall status	$N\bar{K}$	$\Sigma\pi$	Other channels
$\Lambda(1116)$	$1/2^+$	****			$N\pi$ (weak decay)
$\Lambda(1380)$	$1/2^-$	**	**	**	
$\Lambda(1405)$	$1/2^-$	****	****	****	
$\Lambda(1520)$	$3/2^-$	****	****	****	$\Lambda\pi\pi$, $\Lambda\gamma$
$\Lambda(1600)$	$1/2^+$	****	***	****	$\Lambda\pi\pi$, $\Sigma(1385)\pi$
$\Lambda(1670)$	$1/2^-$	****	****	****	$\Lambda\eta$
$\Lambda(1690)$	$3/2^-$	****	****	***	$\Lambda\pi\pi$, $\Sigma(1385)\pi$
$\Lambda(1710)$	$1/2^+$	*	*	*	
$\Lambda(1800)$	$1/2^-$	***	***	**	$\Lambda\pi\pi$, $\Sigma(1385)\pi$, $N\bar{K}^*$
$\Lambda(1810)$	$1/2^+$	***	**	**	$N\bar{K}_2^*$
$\Lambda(1820)$	$5/2^+$	****	****	****	$\Sigma(1385)\pi$
$\Lambda(1830)$	$5/2^-$	****	****	****	$\Sigma(1385)\pi$
$\Lambda(1890)$	$3/2^+$	****	****	**	$\Sigma(1385)\pi$, $N\bar{K}^*$
$\Lambda(2000)$	$1/2^-$	*	*	*	

LIGHT UNFLAVORED MESONS ($S = C = B = 0$)

For $I = 1$ (π, b, ρ, a): $u\bar{d}$, $(u\bar{u} - d\bar{d})/\sqrt{2}$, $d\bar{u}$;
for $I = 0$ ($\eta, \eta', h, h', \omega, \phi, f, f'$): $c_1(u\bar{u} + d\bar{d}) + c_2(s\bar{s})$

See related reviews:

- Form Factors for Radiative Pion and Kaon Decays
- Scalar Mesons below 2 GeV
- $\rho(770)$
- Pseudoscalar and Pseudovector Mesons in the 1400
- $\rho(1450)$ and $\rho(1700)$

$\pi^\pm$	$1^-(0^-)$
π^0	$1^-(0^{-+})$
η	$0^+(0^{-+})$
$f_0(500)$ aka σ; was $f_0(600)$	$0^+(0^{++})$
$\rho(770)$	$1^+(1^{--})$
$\omega(782)$	$0^-(1^{--})$
$\eta'(958)$	$0^+(0^{-+})$
$f_0(980)$	$0^+(0^{++})$
$a_0(980)$	$1^-(0^{++})$
$\phi(1020)$	$0^-(1^{--})$
$h_1(1170)$	$0^-(1^{+-})$
$b_1(1235)$	$1^+(1^{+-})$
$a_1(1260)$	$1^-(1^{++})$
$f_2(1270)$	$0^+(2^{++})$
$f_1(1285)$	$0^+(1^{++})$
$\eta(1295)$	$0^+(0^{-+})$
$\pi(1300)$	$1^-(0^{-+})$
$a_2(1320)$	$1^-(2^{++})$
$f_0(1370)$	$0^+(0^{++})$
$\pi_1(1400)$	$1^-(1^{-+})$
$\eta(1405)$	$0^+(0^{-+})$
$h_1(1415)$ was $h_1(1380)$	$0^-(1^{+-})$
$a_1(1420)$	$1^-(1^{++})$
$f_1(1420)$	$0^+(1^{++})$
$\omega(1420)$	$0^-(1^{--})$
$f_2(1430)$	$0^+(2^{++})$
$a_0(1450)$	$1^-(0^{++})$
$\rho(1450)$	$1^+(1^{--})$
$\eta(1475)$	$0^+(0^{-+})$
$f_0(1500)$	$0^+(0^{++})$

- $f_1(1510)$
- $f_2'(1525)$
- $f_2(1565)$
- $\rho(1570)$
- $h_1(1595)$
- $\pi_1(1600)$
- $a_1(1640)$
- $f_2(1640)$
- $\eta_2(1645)$
- $\omega(1650)$
- $\omega_3(1670)$
- $\pi_2(1670)$
- $\phi(1680)$
- $\rho_3(1690)$
- $\rho(1700)$
- $a_2(1700)$
- $f_0(1710)$
- $\eta(1760)$
- $\pi(1800)$
- $f_2(1810)$
- $X(1835)$
- $\phi_3(1850)$

Dynamically generated resonances

Many suggestions of dynamically generated resonances...

- Oller, Oset, Pelaez, PRL80(1998)
- Ramos, Oset, Nucl. Phys. A635(1998), A725(2003)
- Krehl, Hanhart, Krewald, Speth, Phys. Rev. C62(2000)
- Nieves, Ruiz-Arriola, Phys. Rev. D64(2001)
- Inoue, Vicente-Vacas, Oset, Phys. Rev. D65(2002)
- Epelbaum, Meissner, Nucl. Phys. A725(2003)
- Garcia-Recio, Nieves, Ruiz-Arriola, Phys. Rev. D67(2003)
- Roca, Oset, Singh, Phys. Rev. D72(2005)
- Molina, Nicmorous, Oset, Phys. Rev. D78(2008)
- Geng, Oset, Phys. Rev. D79(2009)
- Alvarez-Ruso, Oller, Alarcon, Phys. Rev. D80(2009)
- Oset, Ramos, EPJA44(2010)

...and a very long list of authors!

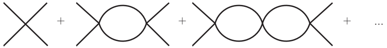

Heavy hadrons

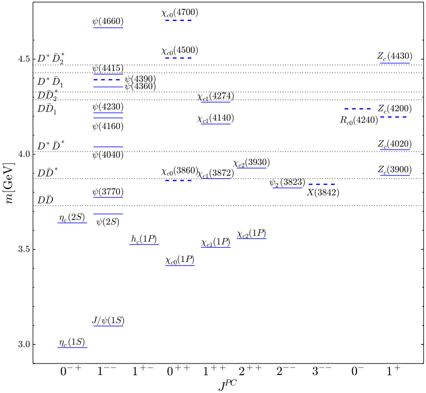

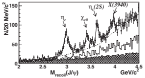

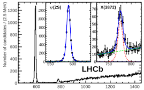

State	M_0 [MeV]	Γ[MeV]
$P_{cs}(4459)^0$	$4458.8 \pm 2.9^{+4.7}_{-1.1}$	$17.3 \pm 6.5^{+8.0}_{-5.7}$

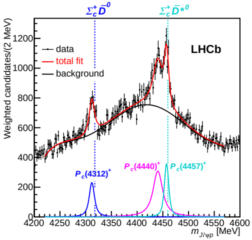

Clear evidence of exotic states!

- **Hidden-charm** charged tetraquarks $Z_c^+ \sim c\bar{d}u\bar{c}$ $(D^{(*)}\bar{D}^{(*)})$.
  Hidden-strange candidate? $a_0(980)$? how many?
- **Hidden-charm** (strange) pentaquarks $P^+_{c(s)} \sim c\bar{c}uud(s)$, $(\bar{D}^{(*)}\Sigma_c^{(*)}(\Xi_c^{(*)}))$.
  Hidden-strange candidate? $N^*(1535)$, (strange) $\Lambda(1405)$,...more?

Nature of the scalar resonances?

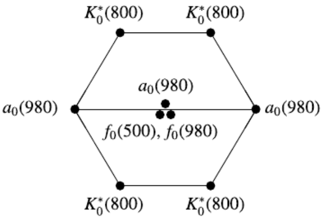

Figure: Light scalar nonet.

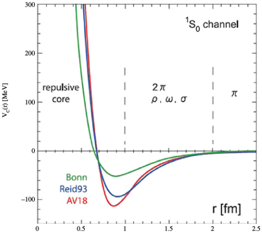

Figure: NN potential ($^1S_0$ channel). The attractive interaction is dominated by the σ or correlated two-pion exchange. PRL99 (2007), Ishii, Aoki.

- 70's. Analyticity, unitarity and crossing symmetry constraints required the existence of a broad σ pole (Guillou, Morel, Navalet, Basdevant, Froggatt, Peterson, Roy).
- Glueball scenario. Not favored by lattice calculations, large N_c arguments and chiral symmetry.
- Alternative scenario to $q\bar{q}$. Jaffe, 1976. MIT bag model, tetraquark?

The σ meson

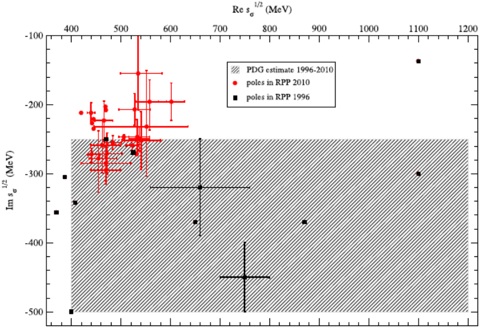

Analyses with Breit-Wigner-like parameterizations led to misleading results (different values of the parameters of the resonance).
Rev. Part. Phys. 1973:

"It is clear that the behavior of the δ_0^0 is much too complicated to allow a description in terms of one or several Breit-Wigner resonances. We therefore list the positions of the poles of the T matrix."

Chiral Perturbation Theory

- ChPT expansion of the amplitude for meson-meson scattering

$$t(s) = t_2(s) + t_4(s) + ...t_{2k} = \mathcal{O}(p^{2k}) \tag{1}$$

- Lowest-order Chiral Lagrangian

$$\mathcal{L}_2 = \frac{f^2}{4}\langle \partial_\mu U^\dagger \partial^\mu U + M(U + U^\dagger)\rangle \tag{2}$$

$$\begin{aligned}
\mathcal{L}_4 = \quad & L_1\langle \partial_\mu U^\dagger \partial^\mu U\rangle^2 + L_2\langle \partial_\mu U^\dagger \partial_\nu U\rangle\langle \partial^\mu U^\dagger \partial^\nu U\rangle \\
& + L_3\langle \partial_\mu U^\dagger \partial^\mu U \partial_\nu U^\dagger \partial^\nu U\rangle + L_4\langle \partial U^\dagger \partial^\mu U\rangle\langle U^\dagger M + M^\dagger U\rangle \\
& + L_5\langle \partial_\mu U^\dagger \partial^\mu U(U^\dagger M + M^\dagger U)\rangle + L_6\langle U^\dagger M + M^\dagger U\rangle^2 \\
& + L_7\langle U^\dagger M - M^\dagger U\rangle^2 + L_8\langle M^\dagger U M^\dagger U + U^\dagger M U^\dagger M\rangle
\end{aligned} \tag{3}$$

Chiral Perturbation Theory

where $U(\phi) = \exp(i\sqrt{2}\Phi/f)$, and

$$\Phi(x) = \left(\begin{array}{ccc} \frac{\pi^0}{\sqrt{2}} + \frac{\eta}{\sqrt{6}} & \pi^+ & K^+ \\ \pi^- & -\frac{\pi^0}{\sqrt{2}} + \frac{\eta}{\sqrt{6}} & K^0 \\ K^- & \bar{K}^0 & -\frac{2}{\sqrt{6}}\eta \end{array} \right)_\mu \tag{4}$$

$$M = \left(\begin{array}{ccc} m_\pi^2 & 0 & 0 \\ 0 & m_\pi^2 & 0 \\ 0 & 0 & 2m_K^2 - m_\pi^2 \end{array} \right) \tag{5}$$

[1] J. Gasser and H. Leutwyler, Annals Phys. **158**, 142 (1984)

[2] J. Gasser and H. Leutwyler, Nucl. Phys. B **250**, 465 (1985)

[3] J. A. Oller, E. Oset and J. R. Pelaez, Phys. Rev. D **59**, 074001 (1999)

Unitarity

- **Unitarity in coupled channels:**

$$\boxed{\mathrm{Im}\, T_{if} = T_{in} \sigma_{nn} T^*_{nf}} \tag{6}$$

with $\sigma_{nn}(s) = -\frac{k_n}{8\pi\sqrt{s}} \theta(s - (m_{1n} + m_{2n})^2)$ and k_n is the on-shell c.m. momentum.

$\sigma = T^{-1} \mathrm{Im}\, T T^{*-1} = \frac{1}{2i} T^{-1}(T - T^*) T^{*-1} = \frac{1}{2i}(T^{-1*} - T^{-1}) = -\mathrm{Im}\, T^{-1}$.

Expansion of T^{-1} in powers of p^2:

$$T^{-1} \simeq T_2^{-1}[1 + T_4 T_2^{-1} + \ldots]^{-1} \simeq T_2^{-1}[1 - T_4 T_2^{-1} \ldots]$$

$$T = T_2 T_2^{-1}[\mathrm{Re}\, T^{-1} - i\sigma]^{-1} T_2^{-1} T_2 = T_2[T_2 \mathrm{Re}\, T^{-1} T_2 - i T_2 \sigma T_2]^{-1} T_2$$

Since $T_2 = \mathrm{Re}\, T_2$, $\mathrm{Im}\, T = \mathrm{Im}\, T_4 = T_2 \sigma T_2$.

$T = [1 - VG]^{-1}$, $V = \frac{V^2}{V_2 - V_4}$; $\mathrm{(Bethe - Salpeter)}$

$$T = T_2[T_2 - \mathrm{Re}\, T_4 - i \mathrm{Im}\, T_4]^{-1} T_2 \longrightarrow \boxed{T = T_2[T_2 - T_4]^{-1} T_2} \tag{7}$$

UChPT (NLO) Oller, Oset, Pelaez (1999) with $T_4 = T_4^p + T_2 G T_2$

Second Riemann Sheet

Schwartz reflexion theorem: $f(z)$ is analytic in a region of the complex plane in which f is real, then

$$f(z^*)^* = f(z) \tag{8}$$

For the loop function, above threshold, $\mathrm{Re}\sqrt{s} > m + M$,

$$G(\sqrt{s} - i\epsilon) = (G(\sqrt{s} + i\epsilon))^* = G(\sqrt{s} + i\epsilon) - i\,2\mathrm{Im}G(\sqrt{s} + i\epsilon) \tag{9}$$

Since the beginning of R2 is equal to the end of R1,

$$G^{II}(\sqrt{s} + i\epsilon) = G^{I}(\sqrt{s} - i\epsilon) = G^{I}(\sqrt{s} + i\epsilon) - i\,2\mathrm{Im}G^{I}(\sqrt{s} + i\epsilon) \tag{10}$$

Since $\mathrm{Im}G^{I}(\sqrt{s} + i\,\epsilon) = -\frac{q}{8\,\pi\sqrt{s}}$,

$$\boxed{G^{II}(\sqrt{s}) = G^{I}(\sqrt{s}) + i\,\frac{q}{4\pi\sqrt{s}}, \quad \mathrm{Im}q > 0} \tag{11}$$

Inverse Amplitude Method

Dispersion relations

$$t(s) = \frac{1}{2\pi i}\int_C \frac{t(s')}{s'-s}ds'$$

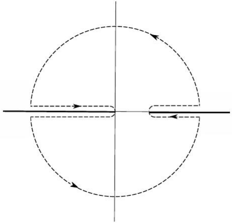

If we assume that $t \to 0$ as $|s| \to \infty$, then

$$\boxed{t(s) = \frac{1}{\pi}\int_{s_{th}}^{\infty}\frac{\mathrm{Im}t(s')}{s'-s}ds' + \frac{1}{\pi}\int_{-\infty}^{0}\frac{\mathrm{Im}t(s')}{s'-s}ds'} \qquad (12)$$

with $\mathrm{Im}t(s+i\epsilon) = \frac{1}{2i}\left[t(s+i\epsilon) - t(s-i\epsilon)\right]$. If t does not goes to zero when $|s| \to \infty$ sufficiently fast,

$$G(s) = \frac{t(s)}{(s-s_1)(s-s_2)....(s-s_N)}$$

Subtraction points: $s_1, s_2, ...s_N$

Inverse Amplitude Method

Dispersion relation of the function $g(s) = t_2(s)^2/t(s)$,

$$g(s) = g(0) + g'(0)\,s + g''(0)s^2 - \frac{s^3}{\pi}\int_{4M_\pi^2}^{\infty} ds'\,\frac{\sigma(s)t_2(s)^2}{s'^{\,3}(s'-s-i\epsilon)}$$
$$+\frac{s^3}{\pi}\int_{-\infty}^{0} ds'\,\frac{\mathrm{Im}\,g(s)}{s'^{\,3}(s'-s-i\epsilon)}, \qquad (13)$$

Subtraction constants. NLO ChPT, $g(0) \simeq t_2(0) - t_4(0)$, $g'(0) \simeq t_2'(0) - t_4'(0)$, $g''(0) \simeq -t_4''(0)$.
Unitarity condition: (physical cut)$\mathrm{Im} g = t_2^2 \mathrm{Im}\frac{1}{t} = -t_2^2\sigma$
Left-hand cut (perturbative expansion)
$\mathrm{Im} g = t_2^2\,\mathrm{Im}\frac{1}{t} \simeq t_2^2\,\mathrm{Im}\frac{1}{t_2+t_4} \simeq -\mathrm{Im} t_4$.

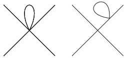

$$\boxed{t_{\mathrm{IAM}}(s) = \frac{t_2(s)^2}{t_2(s) - t_4(s)}}$$

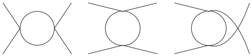

Inverse Amplitude Method

S-matrix

$$S_{ij} = \delta_{ij} + 2\,i\sqrt{\sigma_i \sigma_j}\,t_{ij}, \qquad \sigma_i = \begin{cases} \sqrt{1 - 4\,m_i^2/s} & \sqrt{s} > 2\,m_i \\ 0 & \text{else} \end{cases}$$

Parameterization

$$S = \begin{pmatrix} \eta e^{2i\delta_1} & i(1-\eta^2)^{1/2} e^{i(\delta_1+\delta_2)} \\ i(1-\eta^2)^{1/2} e^{i(\delta_1+\delta_2)} & \eta e^{2i\delta_2} \end{pmatrix}. \tag{14}$$

Analytical continuation,

$$S^I\,(s + i\epsilon) = S^{II}\,(s - i\epsilon)\,. \tag{15}$$

Schwartz reflection principle, i.e. $S\,(s + i\epsilon) = S^*(s - i\epsilon)$;
Unitarity, $SS^* = \mathbb{1} \Longrightarrow S^{II}\,(s - i\epsilon) = S^I\,(s - i\epsilon)^{-1}$. Thus,

$$\boxed{t^{II}(s) = \frac{t^I(s)}{1 + 2\,i\,\sigma(s)\,t^I(s)}} \tag{16}$$

IAM with coupled-channels

Unitarity

$$\mathrm{Im}\, T^{-1} = -\Sigma\,, \quad \Sigma = \begin{pmatrix} \sigma_1 & 0 \\ 0 & \sigma_2 \end{pmatrix}\,, \tag{17}$$

$$T = T_2 \left[T_2 \mathrm{Re} T^{-1} T_2 - i\, T_2 \Sigma T_2 \right]^{-1} T_2\,, \Longrightarrow \boxed{T = T_2 [T_2 - T_4]^{-1} T_2} \tag{18}$$

Riemann sheet n,

$$T^{(n)}(s) = T(s) \left(\mathbb{1} + 2\, i\, \Sigma(s)^{(n)}\, T(s) \right)^{-1}\,, \tag{19}$$

$\pi\pi$, $K\bar{K}$ $I = J = 1$ coupled-channel system,

$$\Sigma^{II} = \begin{pmatrix} \sigma_1 & 0 \\ 0 & 0 \end{pmatrix}, \quad \Sigma^{III} = \begin{pmatrix} 0 & 0 \\ 0 & \sigma_2 \end{pmatrix}, \quad \Sigma^{IV} = \begin{pmatrix} \sigma_1 & 0 \\ 0 & \sigma_2 \end{pmatrix}. \tag{20}$$

Coupling,

$$\boxed{g_i g_j = -16\pi \lim_{s \to s_{\mathrm{pole}}} (s - s_{\mathrm{pole}})\, t_{ij} (2J+1)/2p^{2J}}, \tag{21}$$

Formalism in the finite volume

Two-meson-loop function G:

$$G = G^{co}(E) = \int_{q<q_{max}} \frac{d^3q}{(2\pi)^3} \frac{\omega_1 + \omega_2}{2\omega_1\omega_2} \frac{2M_i}{E^2 - (\omega_1 + \omega_2)^2 + i\epsilon} \qquad (22)$$

where $\omega_i = \sqrt{m_i^2 + |\vec{q}_i\,|^2}$ is the energy and $\vec{q}$ stands for the momentum of the meson in the channel i. In the finite volume, the momenta is quantized,

$$\vec{q}_i = \frac{2\pi}{L}\vec{n}_i; \qquad T \longrightarrow \tilde{T}; \qquad G(E) \longrightarrow \tilde{G}(E)\;, \qquad (23)$$

[1] M. Doring, U. G. Meißner, E. Oset and A. Rusetsky, Eur. Phys. J. A47, 139 (2011)

[2] M. Doring, J. Haidenbauer, U. G. Meißner, and A. Rusetsky, Eur. Phys. J. A47, 163 (2011)

Formalism in the finite volume

$$\tilde{T} = [1 - V\tilde{G}]^{-1} V \qquad (24)$$

with $V = V_2^2/(V_2 - V_4)$, and

$$\tilde{G}(E) = \frac{1}{L^3} \sum_{\vec{q}_i} I(E, \vec{q}_i) \ , \qquad (25)$$

with

$$I(E, \vec{q}_i) = \frac{\omega_1(\vec{q}_i) + \omega_2(\vec{q}_i)}{2\omega_1(\vec{q}_i)\omega_2(\vec{q}_i)} \frac{1}{(E)^2 - (\omega_1(\vec{q}_i) + \omega_2(\vec{q}_i))^2} \qquad (26)$$

and $\vec{q} = \frac{2\pi}{L}(n_x, n_y, n_z)$. The formalism can also be made independent of q_{max} and related to α.

$$\tilde{G} = G^{DR} + \lim_{q_{max}\to\infty} \left(\frac{1}{L^3} \sum_{q<q_{max}} I(E, \vec{q}) - \int_{q<q_{max}} \frac{d^3q}{(2\pi^3)} I(E, \vec{q}) \right)$$

$$\equiv G^{DR} + \lim_{q_{max}\to\infty} \delta G \ , \qquad (27)$$

A. Martinez Torres, L. R. Dai, C. Koren, D. Jido and E. Oset, PRD85(2012)

Formalism in the finite volume

- Bethe-Salpeter eq. finite volume, energy levels:

$$\tilde{T}^{-1} = V^{-1} - \tilde{G} \quad \boxed{\det(I - V\tilde{G}) = 0} \tag{28}$$

- One-channel amplitude inf. volume:

$$T = (\tilde{G}(E_i) - G(E_i))^{-1}. \quad \boxed{\tan\delta = -k/(8\pi E \Delta G)} \tag{29}$$

Boost, Asymmetric Boxes and Partial Wave Decomposition
Doering, Meißner, Oset, Rusetsky (2012)

$$\tilde{T}_{lm,l'm'}(p,p') = V_l(p,p')\delta_{ll'}\delta_{mm'} + \sum_{l''m''} V_l(p,q^{\mathrm{on},*})\tilde{G}_{lm,l''m''}(q^{\mathrm{on},*})\tilde{T}_{l''m'',lm}(q^{\mathrm{on},*},p') \tag{30}$$

$$\boxed{\det(\delta_{ll'}\delta_{mm'} - V_l(q^{\mathrm{on},*},q^{\mathrm{on},*})\tilde{G}_{lm,l'm'}(q^{\mathrm{on},*})) = 0} \tag{31}$$

Irreducible representations for asymmetric boxes and boost $\vec{P} = \frac{2\pi}{\eta L}(0,0,1)$,

$$\mathrm{I} = \mathrm{L} = 0 \longrightarrow \mathrm{A}^+ : -1 + \mathrm{V}_0\mathrm{G}_{00,00} = 0$$

$$\mathrm{I} = \mathrm{L} = 1 \longrightarrow \mathrm{A}_2^- : -1 + \mathrm{V}_1\mathrm{G}_{10,10} = 0; \mathrm{E}^- : -1 + \mathrm{V}_1\mathrm{G}_{11,11} = 0$$

Conformal mapping

Parameterization

- Most general form of the K-matrix as an analytical function of energy
- The convergence of the series is improved by mapping it onto the interior of a disk

$$\omega^{[\mathrm{cm1}]}(s) = \frac{\sqrt{s} - \alpha\sqrt{4m_K^2 - s}}{\sqrt{s} + \alpha\sqrt{4m_K^2 - s}}, \tag{32}$$

$$\omega^{[\mathrm{cm2}]}(s) = \frac{\sqrt{s} - \alpha}{\sqrt{s} + \alpha}, \tag{33}$$

with $\alpha = 1$; $m_K = 550\,\mathrm{MeV}$ [cm1] and $\alpha = 1000$ MeV [cm2].

I. Caprini. Phys. Rev. D77 (2008)

Conformal mapping

***K* matrix**:

$$\boxed{K_{00}^{-1}(s) = \frac{1}{16\pi}\frac{M_\pi^2}{s_A - s}\left(\frac{2s_A}{M_\pi\sqrt{s}} + B_0 + B_1\omega(s) + ...\right)} \tag{34}$$

Chiral symmetry dictates that $T_{00}(s)$ must vanish for $s = s_A \sim M_\pi^2/2$.

- α is fixed (not significant improved if running).
- Two fitting parameters, B_0 and B_1.

Scattering amplitude in the finite volume and $I = L = 0$ channel,

$$\tilde{T}_{00}(s) = \frac{1}{K_{00}^{-1}(s) - \tilde{G}(s)}\ , \tag{35}$$

Solution: Energies E_0^i with covariance matrix C,

$$\boxed{\chi^2 = (E - E_0)^T \cdot C^{-1} \cdot (E - E_0)} \tag{36}$$

which provide a minimal χ^2.

Conformal mapping vs. UChPT fits

Par.	Fitted data set	$M_\pi = 227$ MeV			$M_\pi = 315$ MeV		
		Rez_0	- Imz_0	g	Rez_0	- Imz_0	g
cm1	σ_{227}	460^{+30}_{-60}	180^{+30}_{-30}	$3.2^{+0.1}_{-0.1}$	–	–	–
	σ_{315}	–	–	–	660^{+50}_{-70}	150^{+40}_{-50}	$4.0^{+0.2}_{-0.2}$
cm2	σ_{227}	475^{+30}_{-60}	176^{+50}_{-40}	$3.3^{+0.3}_{-0.2}$	–	–	–
	σ_{315}	–	–	–	660^{+50}_{-90}	140^{+40}_{-50}	$3.9^{+0.2}_{-0.2}$
chm2	σ_{227} ρ_{227}	460^{+30}_{-40}	160^{+30}_{-30}	$3.0^{+0.1}_{-0.1}$	–	–	–
	σ_{315} ρ_{315}	–	–	–	660^{+40}_{-60}	120^{+40}_{-40}	$3.6^{+0.1}_{-0.1}$

Table: Pole positions (z_0 in MeV) and corresponding couplings to $\pi\pi$ channel (g in GeV) in the conformal mapping parameterizations, [cm1] and [cm2], and in the UChPT individual fits [chm2].

Lattice data from GWU 2018 simulation, $m_\pi = 227$ and 315 MeV,
Alexandru, Guo, Molina, Mai, Döring, PRD98(2018)

Conformal mapping vs. UChPT $\sigma + \rho$ individual fits:

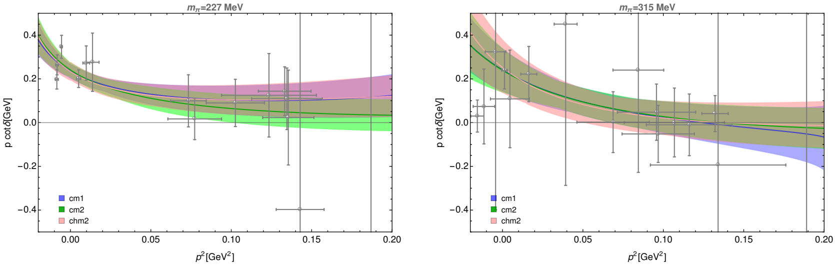

Figure: $p\cot\delta$ as a function of p^2 in the conformal parameterizations for the $I = L = 0$ channel, [cm1] and [cm2], in comparison with the individual $\sigma + \rho$ UChPT fits.

Combined fits from UChPT

σ [chm1] and $\sigma + \rho$ [chm2] fits

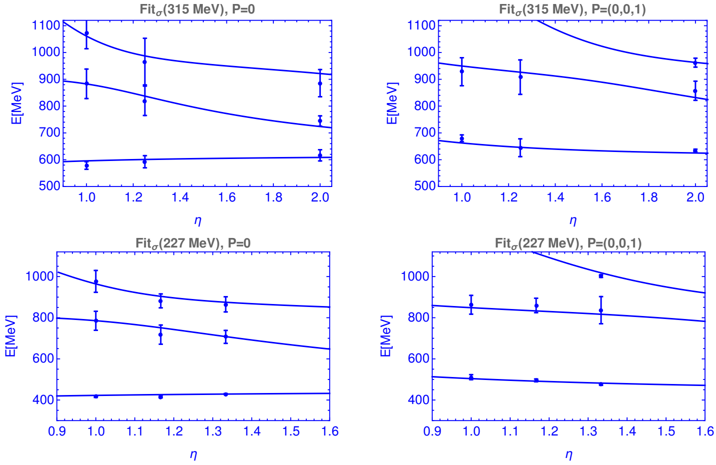

Figure: Energy levels in the σ fits [chm1] to $m_\pi = 227, 315$ MeV energy levels. The energy levels are similar when the ρ meson is included [chm2].

Pion mass dependence

Pole position z_0

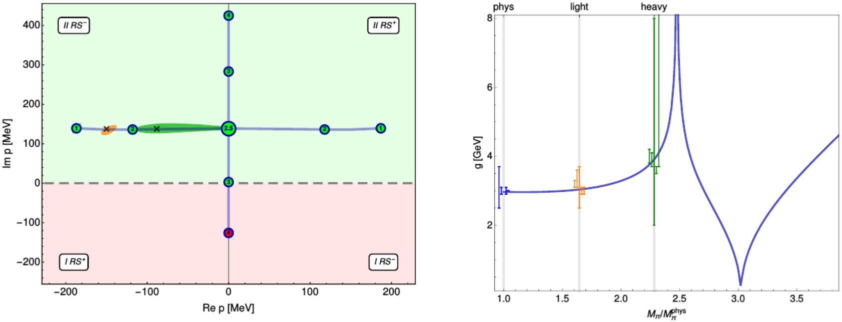

Figure: Left: M_π dependence of the pole position of the σ resonance in the complex plain of the energy. The encircle numbers represent the pion mass in units of the physical one. Right: M_π dependence of the coupling of the σ resonance.

Physical point vs. other works

Par.	$M_\pi = 138$ MeV		
Fitted data set	$\mathrm{Re}z_0$	$-\mathrm{Im}z_0$	g
chm1 $\sigma_{227,315}$	440^{+60}_{-90}	240^{+20}_{-50}	$3.0^{+0.2}_{-0.6}$
chm2 $\sigma_{227,315}$ $\rho_{227,315}$	440^{+10}_{-16}	240^{+20}_{-20}	$3.0^{+0.0}_{-0.0}$
Pelaez 2015	449^{+22}_{-16}	275^{+12}_{-12}	$3.5^{+0.3}_{-0.2}$
Albaladejo 2012	440 ± 10	238 ± 10	
Doring, Mai 2016	452^{+1}_{-0}	144^{+0}_{-4}	$2.6^{+0.0}_{-0.0}$

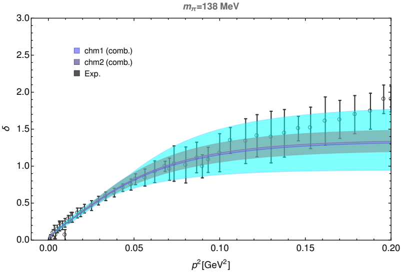

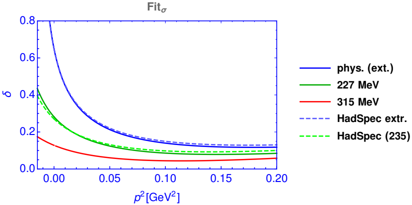

PDG:

Mass: (400 – 550) MeV
Width: (200 – 350) MeV

The ρ meson

- Quark model $\sim q\bar{q}$ meson. Phase shift $\sim$ Breit-Wigner + small corrections, Pisut, Jan and Roos, Matts, Nucl. Phys. B (1968), Lafferty, G. D., Z. Phys. C(1993)
- N_c dependence of the $\rho(770)$ meson leads to small non-$\bar{q}q$ component Pelaez, J. R. and Rios, G. ,PRL (2006), Ruiz de Elvira, J. and Pelaez, PRD(2011)
- Quark-mass dependence of ρ parameters (general Feynmann -Hellmann theorem) requires a non-negligible correction beyond the quark model. Ledwig, T. and Nieves, J. and Pich, A. and Ruiz Arriola, E. and Ruiz de Elvira, J., PRD(2014)
- Dominates the $\pi\pi$ scattering amplitudes in the $I = J = 1$ channel below 1 GeV. Pole parameters have been determined very precisely. Tanabashi, PRD(2018), Ananthanarayan, Colangelo, Gasser, Leutwyler, PR (2001), NPB (2001); Garcia-Martin, Kaminski, Pelaez, Ruiz de Elvira, Yndurain, PRD (2011)
- The $\rho(770)$ contribution is also important for the hadronic total cross section $\sigma(e^+e^- \to \mathrm{hadrons})$, hadronic-vacuum polarization, light-by-light contributions to the anomalous magnetic moment of the muon Aubert, Bernard, Phys. Rev. Lett (2009); Babusci et al. PLB(2012), Ablikim et al. PLB(2015),Eidelman, and Jegerlehner, Phys. C(1995);Jegerlehner Fred and Nyffeler, Andreas, PR (2009); Colangelo, Gilberto and Hoferichter, PRL (2017)
- Role int the restoration of chiral symmetry at higher temperatures Pisarski, Robert PRD (1995); Harada, Masayasu and Yamawaki, Koichi, PRL(2001); Gomez Nicola, Pelaez, Ruiz de Elvira, PRD(2013)

Previous results with UChPT

Analyses $N_f = 2$ & $2+1$ lattice data done in Refs. : Hu, Molina, Döring, Alexandru, PRL 117 (2016), Guo, Alexandru, Molina and M. Döring, PRD(2016) ;Hu, Molina, Doring, Mai, Alexandru, PRD (2017)

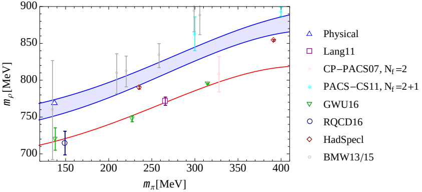

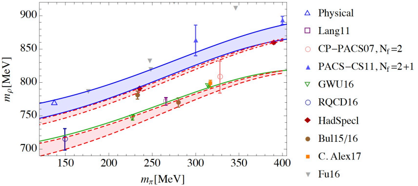

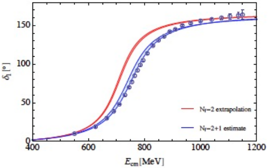

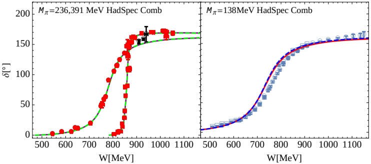

Previous results with UChPT

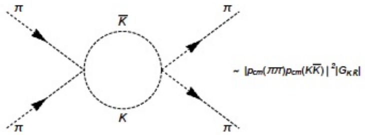

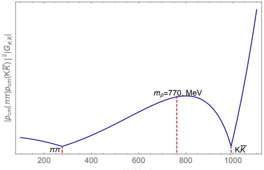

NLO UChPT vs. One-loop UChPT; Not that small!!

Ratio of the couplings of the ρ meson to $\pi\pi$ and $K\bar{K}$

	Oller/Pelaez(1999)	Guo/Oller(2012)
$\frac{g_{K\bar{K}}}{g_{\pi\pi}}$	0.54	0.64

Can this be explained by different values of the strange quark (kaon) mass? (or because of uncertainties in “a”, or both...?)

New $N_f = 2+1$ data on TrM$= K$:

Andersen, Christian and Bulava, John and Hörz, Ben and Morningstar, Colin, NPB(2018)

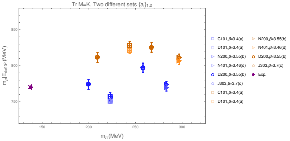

FLAG Review 2019

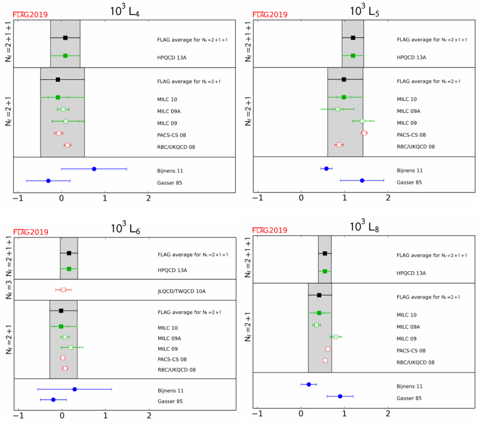

Only based on the trajectory $m_s = m_s^0$ ($0 \equiv$ phys.), no input on the strange quark mass dependence of decay constants.

The FLAG average is not a fit of data (large errors)
Only pseudoscalar masses and decay constant data analyses.

- Analysis of $\pi\pi$ $I = 1, J = 1$ phase shift lattice data (ρ meson) & pseudoscalar meson masses and decay constants on different chiral trajectories ($m_s = m_s^0$ and TrM=TrM^0)
- Check of the KSFR relation, $g_{\rho\pi\pi} = m_\rho/\sqrt{2}f_\pi$

Chiral trajectories (NLO ChPT)

- **Strange quark mass constant**, $m_s = k$:

$$M_{0K}^2 = +\frac{1}{2} M_{0\pi}^2 + k\, B_0 \ ,$$

where $k = m_s^{(0)}$ or $0.6\, m_s^{(0)}$.

- **Light and strange quark mass varies**, $\mathrm{Tr}\, \mathrm{M} = c$:

$$M_{0K}^2 = -\frac{1}{2} M_{0\pi}^2 + c\, B_0 \ ,$$

with $c = 2m_{ud}^{(0)} + m_s^{(0)}$. Predictions for other k's, c's, and:

- **Symmetric**, $m_s = m_{ud}$,

$$M_{0k}^2 = M_{0\pi}^2 \ ,$$

- **Light quark mass constant**, $m_{ud} = m_{ud}^{(0)}$,

$$M_{0\pi}^2 = M_{0\pi}^{2(0)}; M_{0K}^2 = M_{0K}^{2(0)} + (m_s - m_s^{(0)})\, B_0$$

Free parameters: $L_{12} = 2\, L_1 - L_2$ **and** L_i**,** $i = 3, 8$**, and** $c\, B_0$**,** $k\, B_0$**, adjusted to the the chiral trajectories.** $\mu = 770$ **MeV,** $f_0 = 80$ **MeV.**

Fitting procedure

- Energy measurements/phase shifts in the lattice are correlated:

$$\chi_W^2 = (\vec{W}_1 - \vec{W}_0)^T C^{-1} (\vec{W}_1 - \vec{W}_0), \quad W_{1i} = \frac{g(W_{0i}) - f(W_{0i})}{f'(W_{0i}) - g'(W_{0i})} + W_{0i}$$

$\vec{W}_0$: lattice eigenenergies; C: covariance; $\vec{W}_1$: energies of the fit function. Taylor expansion (first order) around W_{0i} for $\delta_L = g(W)$, and $\delta_{\rm fit} = f(W_{1i})$, ($W_{1i}$ =reconstructed energies (Lüscher)).

$$\boxed{\chi = \chi_W^2 + \chi_f^2 + \lambda \sum_{ij} \int |(S\,S^\dagger)_{ij} - \delta_{ij}|^2\, dE}, \quad \chi_f^2 = \sum_{ij} (h_{ij} - h_{ij}^l)^2 / e_{ij}^{l\,2}$$

$h_1 = m_\pi / f_\pi$, $h_2 = m_K / f_K$ and $h_3 = m_K / f_\pi$.
Molina, Ruiz de Elvira, JHEP2011(2020)

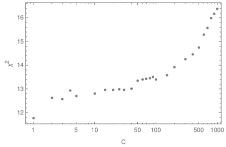

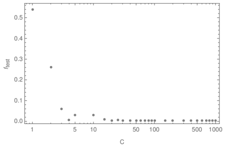

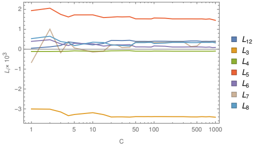

NLO Chiral fits

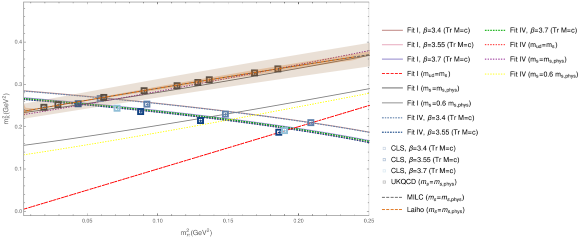

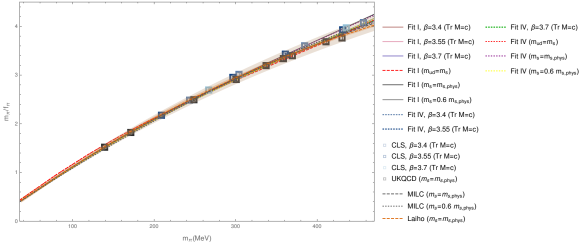

LEC $\times 10^3$	Fit I
L_4	$-0.06(1)$
L_5	$0.91(2)$
L_6	$0.15(2)$
L_8	$0.03(3)$
$c(k)\, B_0 \times 10^{-3}(\mathrm{MeV}^2)$	Fit I
$[c\, B_0]_{\beta=3.4}$	316(6)
$[c\, B_0]_{\beta=3.55}$	295(6)
$[c\, B_0]_{\beta=3.7}$	298(6)
$[k\, B_0]_{m_{s,\mathrm{phys}}}$	257(6)

$$\Sigma_0 = B_0 f_0^2 = -\langle 0|\bar{q}q|0\rangle_0 \Longrightarrow$$

$$\boxed{\Sigma_0^{1/3} = 245 - 280 MeV}$$

Flag review: 214 — 290 MeV.

MILC: $\Sigma_0^{1/3} = 245(5)(4)(4)$ MeV.

We obtain 258 and 245 MeV for Fits I and IV in the $m_s = m_{s,\mathrm{phys}}$ trajectory, respectively, which are compatible.

Global fit decay constant + phase shift lattice data

$(\chi^2/\mathrm{d.o.f} = 1.2)$	LECs $\times 10^3$
L_{12}	$0.36^{+0.02(0.06)}_{-0.02(0.02)}$
L_3	$-3.44^{+0.04(0.07)}_{-0.04(0.06)}$
L_4	$-0.08^{+0.03(0.05)}_{-0.04(0.03)}$
L_5	$0.98^{+0.07(0.06)}_{-0.05(0.04)}$
L_6	$0.24^{+0.08(0.16)}_{-0.06(0.05)}$
L_7	$0.008^{+0.09(0.12)}_{-0.14(0.15)}$
L_8	$0.098^{+0.10(0.11)}_{-0.11(0.16)}$
	$c(k) \times 10^{-3}$ (MeV^2)
Tr $MB_0(\beta = 3.4)$	$268^{+14(8)}_{-18(20)}$
Tr $MB_0(\beta = 3.55)$	$254^{+11(7)}_{-18(18)}$
Tr $MB_0(\beta = 3.7)$	$257^{+12(7)}_{-17(19)}$
$m_s B_0$	$224^{+14(10)}_{-18(20)}$

Table: Values of the parameters obtained in Fit IV.

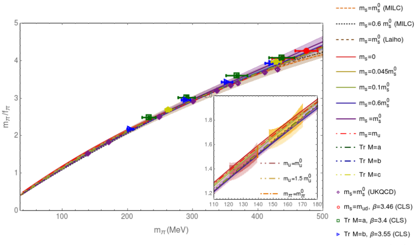

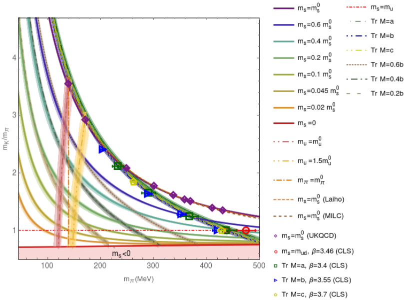

Global fit decay constant + phase shift lattice data

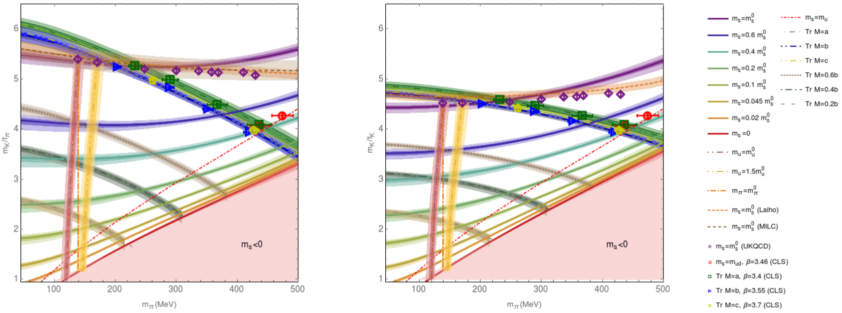

Figure: Decay constant ratios, m_K/f_π and m_K/f_K, obtained in Fit IV in comparison with the lattice data.

Global fit decay constant + phase shift lattice data

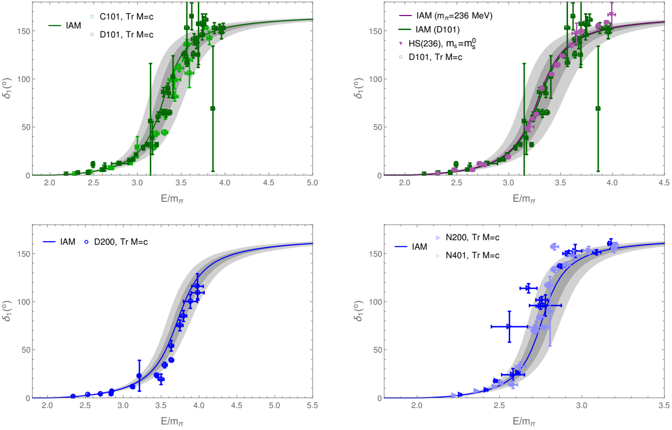

Figure 12: Phase shift lattice data for the trajectories Tr M$=c$ in comparison with the result of the global fit ($m_\pi \simeq 200, 230$ and 280 MeV, D200, D101 and N200 respectively).

Global fit decay constant + phase shift lattice data

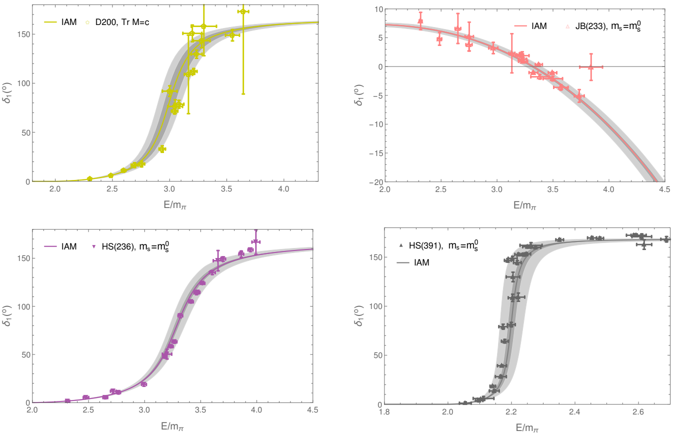

Figure 13: Phase shift lattice data for the trajectories Tr M$=c$ ($m_\pi \simeq 260$ MeV), and $m_s = m_s^0$, in comparison with the result of the global fit.

Global fit decay constant + phase shift lattice data

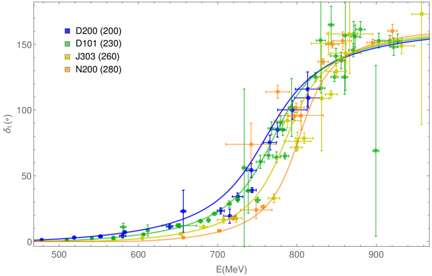

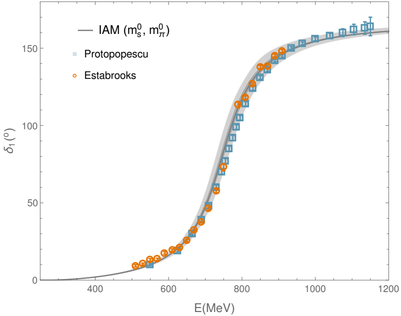

Figure 14: Phase shift lattice data for the trajectories Tr M$=c$, and extrapolation to the physical point in comparison with experimental data.

Global fit decay constant + phase shift lattice data

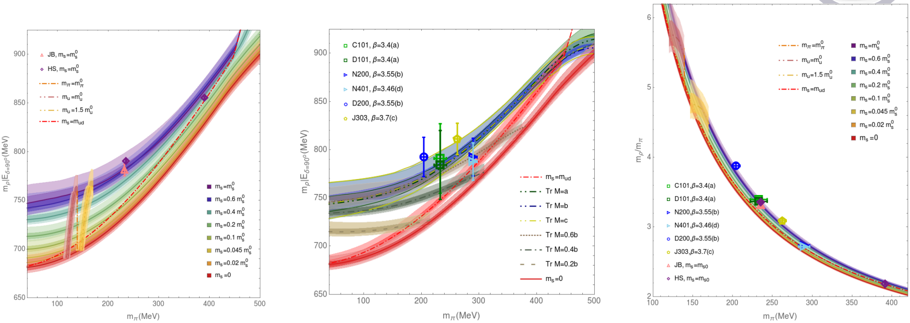

Figure 15: Result of the global fit for M_ρ over trajectories $m_s = k$ and TrM$= c$, in comparison with lattice data.

- $M_\rho(m_\pi)$ becomes flatter in TrM$= c$ trajectories.
- Around $m_\pi = 450$ MeV, the ρ becomes bounds in near $m_s = m_s^0$ trajectories, while it starts to decay into $K\bar{K}$ in the TrM$= c$ ones.
- In the chiral limit the mass of the ρ is $\simeq 680$ MeV.

Global fit decay constant + phase shift lattice data

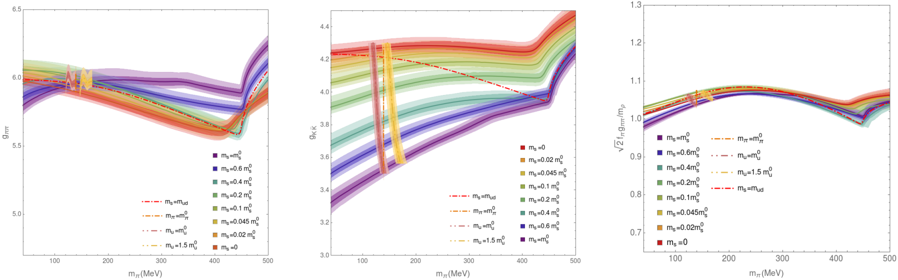

Figure 16: $g_{\pi\pi}$, $g_{K\bar{K}}$ and the ratio $\sqrt{2}f_\pi g_{\pi\pi}/m_\rho$ (KSFR).

- The coupling to $K\bar{K}$ increases when m_s becomes lighter.
- The ratio of the couplings becomes $g_{K\bar{K}}/g_{\pi\pi} = 1/\sqrt{2}$ in the symmetric line.
- The ρ becomes bound for m_π around 430 MeV

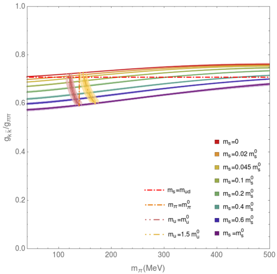

Global fit decay constant + phase shift lattice data

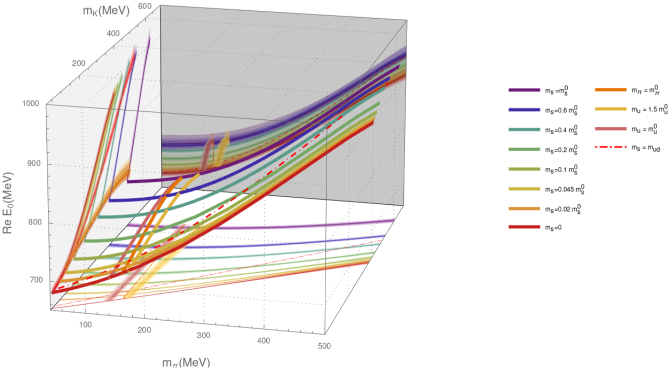

Figure 17: Real part of the pole position of the rho meson.

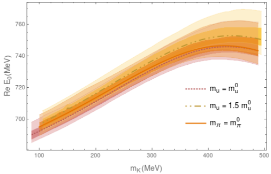

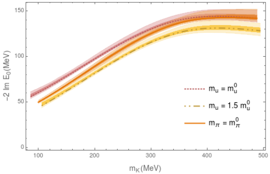

Figure 18: Re(Im)$\sqrt{s_0}$ as a function of m_K over the $m_u = c$, $m_\pi = m_\pi^0$ trajectories.

Global fit decay constant + phase shift lattice data

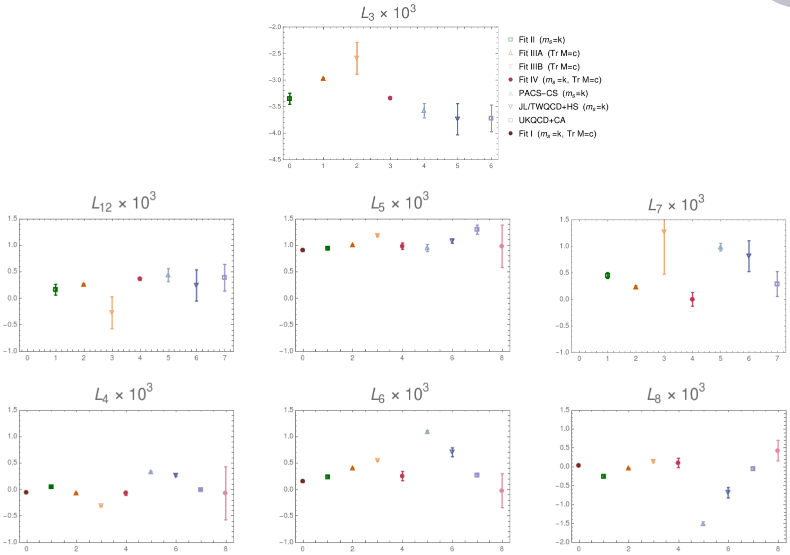

Comparison with $N_f = 2$ and $N_f = 2+1+1$ lattice data

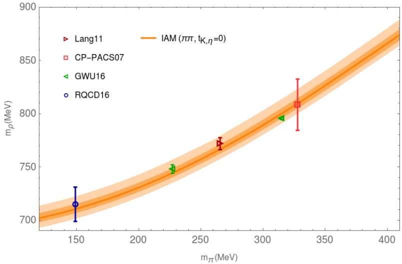

Figure 20: Result for the ρ meson mass when interacting terms involving kaons and etas are set to zero in comparison with $N_f = 2$ lattice data.

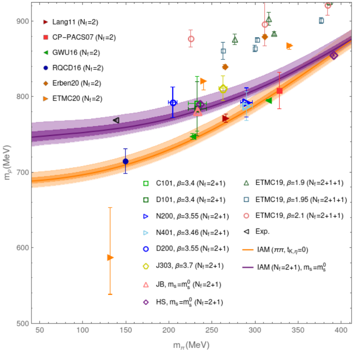

Figure 21: Comparison of $N_f = 2+1$ with new $N_f = 2$ and $N_f = 2+1+1$ data.

The hidden gauge formalism

Bando, Kugo, Yamawaki, PRL54,1215

Lagrangian

$$\mathcal{L} = \mathcal{L}^{(2)} + \mathcal{L}_{III} \tag{37}$$

$$\begin{aligned} \mathcal{L}^{(2)} &= \frac{1}{4} f^2 \langle D_\mu U D^\mu U^\dagger + \chi U^\dagger + \chi^\dagger U \rangle \\ \mathcal{L}_{III} &= -\frac{1}{4} \langle V_{\mu\nu} V^{\mu\nu} \rangle + \frac{1}{2} M_V^2 \langle [V_\mu - \frac{i}{g} \Gamma_\mu]^2 \rangle \\ D_\mu U &= \partial_\mu U - ieQA_\mu U + ieUQA_\mu, \qquad U = e^{i\sqrt{2}P/f} \end{aligned} \tag{38}$$

Upon expansion of $[V_\mu - \frac{i}{g}\Gamma_\mu]^2$, $\mathcal{L}'s$

$$\mathcal{L}_{V\gamma} = -M_V^2 \frac{e}{g} A_\mu \langle V^\mu Q \rangle, \mathcal{L}_{VPP} = -ig \langle V^\mu [P, \partial_\mu P] \rangle, \mathcal{L}_{\gamma PP} = ieA_\mu \langle Q[P, \partial_\mu P] \rangle, \ldots$$

$$\frac{F_V}{M_V} = \frac{1}{\sqrt{2}g}, \qquad \frac{G_V}{M_V} = \frac{1}{2\sqrt{2}g}, \qquad F_V = \sqrt{2}f, \qquad G_V = \frac{f}{\sqrt{2}}, \qquad g = \frac{M_V}{2f}$$

Vector-vector scattering Bando,Kugo,Yamawaki

$$\boxed{\mathcal{L}_{III} = -\frac{1}{4}\langle V_{\mu\nu} V^{\mu\nu}\rangle} \longrightarrow \boxed{\mathcal{L}_{III}^{(3V)} = ig\langle(\partial_\mu V_\nu - \partial_\nu V_\mu) V^\mu V^\nu\rangle}$$

$$\boxed{\mathcal{L}_{III}^{(c)} = \frac{g^2}{2}\langle V_\mu V_\nu V^\mu V^\nu - V_\nu V_\mu V^\mu V^\nu\rangle}$$

$$V_{\mu\nu} = \partial_\mu V_\nu - \partial_\nu V_\mu - ig[V_\mu, V_\nu]$$
$$g = \frac{M_V}{2f}$$

$$V_\mu = \begin{pmatrix} \frac{\rho^0}{\sqrt{2}} + \frac{\omega}{\sqrt{2}} & \rho^+ & K^{*+} & \bar{D}^{*0} \\ \rho^- & -\frac{\rho^0}{\sqrt{2}} + \frac{\omega}{\sqrt{2}} & K^{*0} & D^{*-} \\ K^{*-} & \bar{K}^{*0} & \phi & D_s^{*-} \\ D^{*0} & D^{*+} & D_s^{*+} & J/\psi \end{pmatrix}_\mu$$

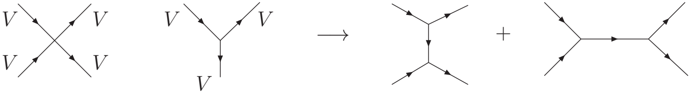

a) b) c) d)

PB and VB interaction

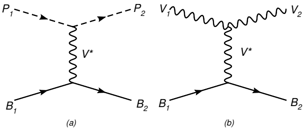

$$\mathcal{L}_{BBV} = g(\langle \bar{B}\gamma_\mu [V^\mu, B]\rangle + \langle \bar{B}\gamma_\mu B\rangle\langle V^\mu\rangle)$$
$$t_{P_1 P_2 V} = g_{15_F} C_{15_F}(15 \otimes 15)\,(q_1 + q_2)_\mu \epsilon^\mu$$
$$t_{B_1 \bar{B}_2 V} = \{g_{15_1}\, C_{15_1}(20' \otimes \bar{20}') + g_{15_2}\, C_{15_2}(20' \otimes \bar{20}')$$
$$+ g_1\, C_1(20' \otimes \bar{20}')\}\bar{u}_{r'}(p_2)\gamma \cdot \epsilon\, u_r(p_1)$$

with $g_{15_F} = -2\sqrt{2}g$. g_{15_1}, g_{15_2} and g_1 are evaluated demanding

1) The couplinga $p\bar{p} \to J/\psi$, $p\bar{p} \to \phi$ should be zero by OZI rules,
2) The coupling $p\bar{p} \to \rho^0$ should be the one obtained in SU(3).

$$g_{15_1} = -g; \qquad g_{15_2} = 2\sqrt{3}\,g; \qquad g_1 = 3\sqrt{5}\,g\ .$$

Bethe-Salpeter equation

$$\boxed{T = [I - VG]^{-1}\, V}$$

Pentaquark states

Wu, Molina, Oset, Zou (2010)

$$V_{ab(P_1 B_1 \to P_2 B_2)} = \frac{C_{ab}}{4f^2}(q_1^0 + q_2^0)$$

$$V_{ab(V_1 B_1 \to V_2 B_2)} = \frac{C_{ab}}{4f^2}(q_1^0 + q_2^0)\vec{\epsilon}_1 \cdot \vec{\epsilon}_2$$

	$\bar{D}^*\Sigma_c$	$\bar{D}^*\Lambda_c^+$	ρN	ωN	ϕN	$K^*\Sigma$	$K^*\Lambda$
$\bar{D}^*\Sigma_c$	-1	0	$-1/2$	$\sqrt{3}/2$	0	1	0
$\bar{D}^*\Lambda_c^+$		1	$-3/2$	$-\sqrt{3}/2$	0	0	1

C_{ab} for the VB system in the sector $I = 1/2$, $S = 0$.

	$\bar{D}_s^*\Lambda_c^+$	$\bar{D}^*\Xi_c$	$\bar{D}^*\Xi_c'$	$\rho\Sigma$	$\omega\Lambda$	$\phi\Lambda$	$\bar{K}^*N$	$K^*\Xi$
$\bar{D}_s^*\Lambda_c^+$	0	$-\sqrt{2}$	0	0	0	-1	$-\sqrt{3}$	0
$\bar{D}^*\Xi_c$		-1	0	$-3/2$	$-1/2$	0	0	$\sqrt{3/2}$
$\bar{D}^*\Xi_c'$			-1	$\sqrt{3}/2$	$\sqrt{3}/2$	0	0	$1/\sqrt{2}$

C_{ab} for the VB system in the sector $I = 0$, $S = -1$.

PB resonances (units in MeV)

(I, S)	M	Γ	Γ_i					
$(1/2, 0)$			πN	ηN	$\eta' N$	$K\Sigma$		$\eta_c N$
	4261	56.9	3.8	8.1	3.9	17.0		23.4
$(0, -1)$			$\bar{K}N$	$\pi\Sigma$	$\eta\Lambda$	$\eta'\Lambda$	$K\Xi$	$\eta_c\Lambda$
	4209	32.4	15.8	2.9	3.2	1.7	2.4	5.8
	4394	43.3	0	10.6	7.1	3.3	5.8	16.3

VB resonances

(I, S)	M	Γ	Γ_i					
$(1/2, 0)$			ρN	ωN	$K^*\Sigma$			$J/\psi N$
	4412	47.3	3.2	10.4	13.7			19.2
$(0, -1)$			$\bar{K}^*N$	$\rho\Sigma$	$\omega\Lambda$	$\phi\Lambda$	$K^*\Xi$	$J/\psi\Lambda$
	4368	28.0	13.9	3.1	0.3	4.0	1.8	5.4
	4544	36.6	0	8.8	9.1	0	5.0	13.8

$\Lambda_b \to p + J/\psi + K^-$

Experimental P_c states (LHCb, 2019)

M (MeV)	Γ (MeV)
$4311.9 \pm 0.7^{+6.8}_{-0.6}$	$9.8 \pm 2.7^{+3.7}_{-4.5}$
$4440.3 \pm 1.3^{+4.1}_{-4.7}$	$20.6 \pm 4.9^{+8.7}_{-10.1}$
$4457.3 \pm 0.6^{+4.1}_{-1.7}$	$6.4 \pm 2^{+5.7}_{-1.9}$
P_{cs} states (LHCb, 2020)	
$4458.8 \pm 2.9^{+4.7}_{-1.1}$	$17.3 \pm 6.5^{+8.0}_{-5.7}$

Pentaquarks states

LHCb 2015.

$P_c^+(4380)$, $M = (4380 \pm 8 \pm 29)$ MeV, $\Gamma = (205 \pm 18 \pm 86)$ MeV, and
$P_c^+(4450)$, $M = (4449.8 \pm 1.7 \pm 2.5)$ MeV, $\Gamma = (39 \pm 5 \pm 19)$ MeV
Assignments: $(3/2^+, 5/2^-)$ and $(5/2^+, 3/2^-)$ are possible.

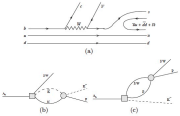

FIG. 1: Mechanisms for the $\Lambda_b \to J/\psi K^- p$ reaction implementing the final state interaction

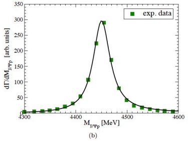

FIG. 2: Results for the K^-p and $J/\psi\, p$ invariant mass distributions compared to the data of ref. [24].

The theoretical analysis of the $\Lambda_b \to J/\psi K^- p$ L. Roca, J. Nieves and E. Oset, PRD92, 094003(2015) supports the $J^P = 3/2^-$ assignment of the pentaquark state, and its nature as $\bar{D}^*\Sigma_c$, $\bar{D}^*\Sigma_c^*$ molecule.

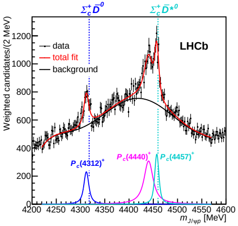

In 2019 the new experimental analysis shows one more pentaquark, $P_c(4312)$ and $P_c(4450)$ splits into two.

Pentaquark states

Generalized HGF formalism with HQSS Xiao, Nieves, Oset (2013,2019)

$I = 1/2$; $C = 0$; $S = -1$; $J^P = 1/2^-$

	$J/\psi\Lambda$	$\bar{D}^*\Xi_c$	$\bar{D}_s^*\Lambda_c$	$\bar{D}^*\Xi'_c$	$\bar{D}\Xi_c^*$	$\bar{D}^*\Xi_c^*$
$4429.52 + i7.67$						
$\lvert g_i \rvert$	0.32	**2.77**	0.74	0.02	0.06	0.04
$4506.99 + i1.03$						
$\lvert g_i \rvert$	0.27	0.03	0.03	0.03	**1.56**	0.05

$I = 1/2$; $C = 0$; $S = 0$; $J^P = 1/2^-$

$(4306.38 + i7.62)$							
	$\eta_c N$	$J/\psi N$	$\bar{D}\Lambda_c$	$\bar{D}\Sigma_c$	$\bar{D}^*\Lambda_c$	$\bar{D}^*\Sigma_c$	$\bar{D}^*\Sigma_c^*$
$\lvert g_i \rvert$	0.67	0.46	0.01	2.09	0.25	0.31	0.16
$(4452.96 + i11.72)$							
	$\eta_c N$	$J/\psi N$	$\bar{D}\Lambda_c$	$\bar{D}\Sigma_c$	$\bar{D}^*\Lambda_c$	$\bar{D}^*\Sigma_c$	$\bar{D}^*\Sigma_c^*$
$\lvert g_i \rvert$	0.25	0.89	0.11	0.13	0.14	2.03	0.19

$I = 1/2$; $C = 0$; $S = 0$; $J^P = 3/2^-$

$(4374.33 + i6.87)$	$J/\psi N$	$\bar{D}^*\Lambda_c$	$\bar{D}^*\Sigma_c$	$\bar{D}\Sigma_c^*$	$\bar{D}^*\Sigma_c^*$
$\lvert g_i \rvert$	0.73	0.18	0.19	1.94	0.30
$(4452.48 + i1.49)$	$J/\psi N$	$\bar{D}^*\Lambda_c$	$\bar{D}^*\Sigma_c$	$\bar{D}\Sigma_c^*$	$\bar{D}^*\Sigma_c^*$
$\lvert g_i \rvert$	0.30	0.07	1.82	0.08	0.19

Mass	Width	Main channel	J^P	Experiment
4306.4	15.2	$\bar{D}\Sigma_c$	$1/2^-$	$P_c(4312)$
4453.0	23.4	$\bar{D}^*\Sigma_c$	$1/2^-$	$P_c(4440)$
4452.5	3.0	$\bar{D}^*\Sigma_c$	$3/2^-$	$P_c(4457)$

The heavy quarks are spectators if we exchange light vectors. Heavy quark spin symmetry is automatically fulfilled.
The exchange of light vectors gives the dominant terms.

New flavor exotic tetraquark

LHCb (2020): Two states $J^P = 0^+, 1^-$ decaying to $D\bar{K}$ ($\bar{D}K$ in the experiment). First clear example of an heavy-flavor exotic tetraquark, $\sim cs\bar{u}\bar{d}$ $(C = 1, S = -1)$.

$$X_0(2866): M = 2866 \pm 7 \quad \text{and} \quad \Gamma = 57.2 \pm 12.9\,\mathrm{MeV},$$
$$X_1(2900): M = 2904 \pm 5 \quad \text{and} \quad \Gamma = 110.3 \pm 11.5\,\mathrm{MeV}.$$

Molina,Branz,Oset, PRD82(2010). HGF

J	Amplitude	Contact	V-exchange	$\sim$ Total
0	$D^*\bar{K}^* \to D^*\bar{K}^*$	$4g^2$	$-\frac{g^2(p_1+p_4).(p_2+p_3)}{m^2_{D_s^*}} + \frac{1}{2}g^2(\frac{1}{m^2_\omega} - \frac{3}{m^2_\rho})(p_1+p_3).(p_2+p_4)$	$-9.9g^2$
1	$D^*\bar{K}^* \to D^*\bar{K}^*$	0	$\frac{g^2(p_1+p_4).(p_2+p_3)}{m^2_{D_s^*}} + \frac{1}{2}g^2(\frac{1}{m^2_\omega} - \frac{3}{m^2_\rho})(p_1+p_3).(p_2+p_4)$	$-10.2g^2$
2	$D^*\bar{K}^* \to D^*\bar{K}^*$	$-2g^2$	$-\frac{g^2(p_1+p_4).(p_2+p_3)}{m^2_{D_s^*}} + \frac{1}{2}g^2(\frac{1}{m^2_\omega} - \frac{3}{m^2_\rho})(p_1+p_3).(p_2+p_4)$	$-15.9g^2$

Table: Tree level amplitudes for $D^*\bar{K}^*$ in $I = 0$. The last column shows the value of V at threshold.

New flavor exotic tetraquark

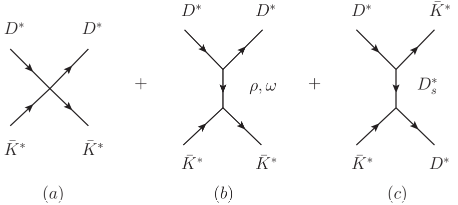

$$\mathcal{P}^{(0)} = \frac{1}{3}\epsilon_\mu\epsilon^\mu\epsilon_\nu\epsilon^\nu$$
$$\mathcal{P}^{(1)} = \frac{1}{2}(\epsilon_\mu\epsilon_\nu\epsilon^\mu\epsilon^\nu - \epsilon_\mu\epsilon_\nu\epsilon^\nu\epsilon^\mu)$$
$$\mathcal{P}^{(2)} = \{\frac{1}{2}(\epsilon_\mu\epsilon_\nu\epsilon^\mu\epsilon^\nu + \epsilon_\mu\epsilon_\nu\epsilon^\nu\epsilon^\mu) - \frac{1}{3}\epsilon_\mu\epsilon^\mu\epsilon_\nu\epsilon^\nu\} \ .$$

States with $C = 1$, $S = 1$, $I = 0$

$I(J^P)$	$M[\mathrm{MeV}]$	$\Gamma[\mathrm{MeV}]$	Channels	state
$0(2^+)$	2572	23	D^*K^* , $D_s^*\phi$, $D_s^*\omega$	$D_{s2}(2572)$
$0(1^+)$	2707	-	D^*K^* , $D_s^*\phi$, $D_s^*\omega$	?
$0(0^+)$	2683	71	D^*K^* , $D_s^*\phi$, $D_s^*\omega$	?

$$\boxed{T = [\hat{1} - VG]^{-1} V}$$

States with $C = 1$, $S = -1$, $I = 0$

$I(J^P)$	$M[\mathrm{MeV}]$	$\Gamma[\mathrm{MeV}]$	Channels	state
$0(2^+)$	2733	36	$D^*\bar{K}^*$	?
$0(1^+)$	2839	-	$D^*\bar{K}^*$	?
$0(0^+)$	2848	59	$D^*\bar{K}^*$	$X_0(2866)$

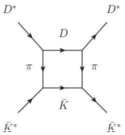

New flavor exotic tetraquark

Two-meson loop function:

$$G_i(s) = \frac{1}{16\pi^2}\left(\alpha + \mathrm{Log}\frac{M_1^2}{\mu^2} + \frac{M_2^2 - M_1^2 + s}{2s}\mathrm{Log}\frac{M_2^2}{M_1^2} + \frac{p}{\sqrt{s}}\left(\mathrm{Log}\frac{s - M_2^2 + M_1^2 + 2p\sqrt{s}}{-s + M_2^2 - M_1^2 + 2p\sqrt{s}} + \mathrm{Log}\frac{s + M_2^2 - M_1^2 + 2p\sqrt{s}}{-s - M_2^2 + M_1^2 + 2p\sqrt{s}}\right)\right),$$

Form factor (box-diagram):

$$F(q) = e^{((p_1^0 - q^0)^2 - \vec{q}^{\,2})/\Lambda^2} \qquad \text{Navarra, PRD65(2002)} \tag{39}$$

with $q_0 = (s + m_D^2 - m_K^2)/2\sqrt{s}$, $\Lambda \sim 1 - 1.3$ GeV. Previous work (2010): $\alpha = -1.6$ (with $\mu = 1500$ MeV) and $\Lambda = 1200$. Recent work: Molina, Oset PLB811 2020, $\alpha = -1.474$, $\Lambda = 1300$.

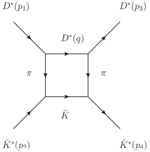

$$\mathcal{L} = \frac{iG'}{\sqrt{2}}\epsilon^{\mu\nu\alpha\beta}\langle\delta_\mu V_\nu \delta_\alpha V_\beta P\rangle$$

$$\mathcal{L}_{VPP} = -ig\langle[P, \partial_\mu P]V^\mu\rangle$$

New flavor exotic tetraquark

$I(J^P)$	$M[\mathrm{MeV}]$	$\Gamma[\mathrm{MeV}]$	Coupled channels	state
$0(2^+)$	2775	38	$D^*\bar{K}^*$	?
$0(1^+)$	2861	20	$D^*\bar{K}^*$	?
$0(0^+)$	2866	57	$D^*\bar{K}^*$	$X_0(2866)$

Table: New results including the width of the D^*K channel.

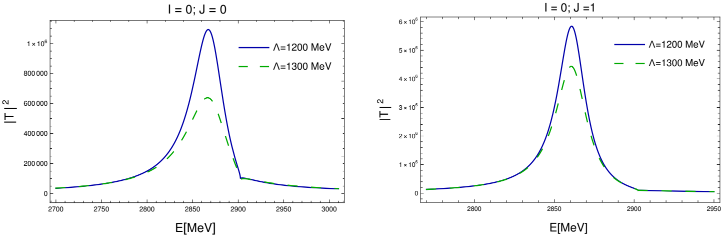

Figure: $|T|^2$ for $C = 1, S = -1, I = 0, J = 0$ and $J = 1$.

Hidden-charm strange tetraquark?

BESIII (2020) has reported a state, $Z_{cs}(3985)$, from the $D_s^{*-} D^0$, $D_s^- D^{*0}$ invariant mass distribution of $e^+e^- \to K^+(D_s^{*-} D^0 + D_s^- D^{*0})$.

$$M = 3982.5^{+1.8}_{-2.6} \pm 2.1 \ \mathrm{MeV}, \quad \Gamma = 12.8^{+5.3}_{-4.4} \pm 3.0 \ \mathrm{MeV}. \qquad (40)$$

7 MeV above the $D_s^{*-} D^0$, $D_s^- D^{*0}$ threshold. It could be the SU(3) partner of the $Z_c(3900)$ state, where a u or d quark has been replaced by an s quark.

$$J/\psi K^- \ (1), \ \ K^{*-}\eta_c \ (2), \ \ \frac{1}{\sqrt{2}}(D_s^- D^{*0} + D_s^{*-} D^0) \ (3)$$

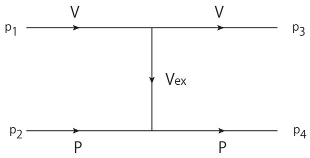

$$\bar{m}_D = 1916 \ \mathrm{MeV}, \bar{m}_{D^*} = 2060 \ \mathrm{MeV}$$

$$A = \frac{1}{\sqrt{2}}(D_s^- D^{*0} + D_s^{*-} D^0),$$

$$B = \frac{1}{\sqrt{2}}(D_s^- D^{*0} - D_s^{*-} D^0).$$

Hidden-charm strange tetraquark?

$$V_{ij} = g^2 C_{ij} \frac{1}{2} \left[3M_{12}^2 - (m_1^2 + m_2^2 + m_3^2 + m_4^2) - \frac{1}{M_{12}^2}(m_1^2 - m_2^2)(m_3^2 - m_4^2) \right],$$

where $M_{12}^2 = (p_1 + p_2)^2$. q^2 correction in the propagators: $q^2 = 0$ for V_{ii} and $q^2 = M^2 + M_{D^*}^2 - 2EM_{D^*}^2$, for V_{13}, V_{23}, with $E = \frac{M_{12}^2 + M^2 - m^2}{2M_{12}}$.

Ikeno, Oset, Molina, PLB(2020)

$$C_{ij} = \begin{pmatrix} 0 & 0 & \frac{\sqrt{2}}{\bar{m}_{D^*}^2} \\ & 0 & \frac{\sqrt{2}}{\bar{m}_{D^*}^2} \\ & & -\frac{1}{m_{J/\psi}^2} \end{pmatrix}.$$

$$T = [1 - VG]^{-1} V,$$

$e^+ e^- \to K^+ (D_s^{*-} D^0 + D_s^- D^{*0})$

$$\boxed{\frac{d\sigma}{dM_{\bar{D}_s D^*}} = \frac{1}{s\sqrt{s}}\, p\tilde{q}\, N\, |T_{33}|^2}$$

$$G_l = \int \frac{d^3 q}{(2\pi)^3} \frac{\omega_1 + \omega_2}{2\omega_1 \omega_2} \frac{1}{(P^0)^2 - (\omega_1 + \omega_2)^2 + i\epsilon}$$

$\omega_1 = \sqrt{m^2 + \vec{q}^{\,2}}$, $\omega_2 = \sqrt{M^2 + \vec{q}^{\,2}}$, and $|\vec{q}| < q_{\rm max}$. $q_{\rm max} \sim$ 700–850 MeV in

Aceti,Oset, PRD90(2014) BS factor, $\psi = -\frac{1}{3} + \frac{4}{3}\left(\frac{m_L}{m_H}\right)^2$ (2.8)

$$p = \frac{\lambda^{1/2}(s, m_K^2, M_{\bar{D}_s D^*}^2)}{2\sqrt{s}},$$

$$\tilde{q} = \frac{\lambda^{1/2}(M_{\bar{D}_s D^*}^2, m_{\bar{D}_s}^2, m_{D^*}^2)}{2M_{\bar{D}_s D^*}},$$

Hidden-charm strange tetraquark?

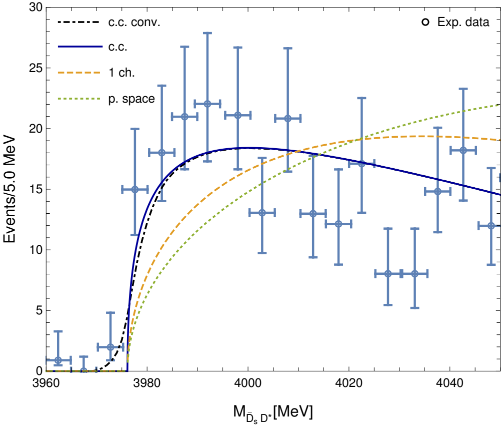

Figure: Results of $d\sigma/dM_{\bar{D}_s D^*}$. Solid line: Result for the $\bar{D}_s D^* + \bar{D}_s^* D$ combination with its coupled channels (c.c.). Dashed line: Result for the single channel $\bar{D}_s D^* - \bar{D}_s^* D$ combination (1 ch.). Dotted line: phase space. Dashed-dotted line: result folded with the experimental resolution (c.c. conv.).

Search for hidden-charm pentaquarks

Stimulated by LHCb, BESIII is conducting an analysis for the search of hidden-strange pentaquarks (decaying to $p\phi$) in Λ_c decays.

- 2014. BESIII collected 567 pb^{-1} close to $\Lambda_c\bar{\Lambda}_c$ production threshold (4.6 GeV). However the result is limited by statistics and no evidence of a peak was found.
- 2020. BESIII has collected new data between 4.6 – 4.7 GeV in 2020.

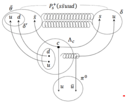

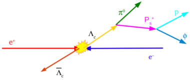

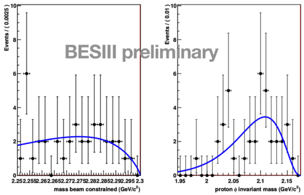

New decay mode $p\phi$

Particle	J^P	overall	Status as seen in $N\gamma$	$N\pi$	$\Delta\pi$	$N\sigma$	$N\eta$	ΛK	ΣK
N	$1/2^+$	****							
$N(1440)$	$1/2^+$	****	****	****	****	***			
$N(1520)$	$3/2^-$	****	****	****	****	**	****		
$N(1535)$	$1/2^-$	****	****	****	***	*	****		
$N(1650)$	$1/2^-$	****	****	****	***	*	****	*	
$N(1675)$	$5/2^-$	****	****	****	****	***	*	*	*
$N(1680)$	$5/2^+$	****	****	****	****	***	*	*	*
$N(1700)$	$3/2^-$	***	**	***	***	*	*		
$N(1710)$	$1/2^+$	****	****	****	*		***	**	*
$N(1720)$	$3/2^+$	****	****	****	***	*	*	****	*
$N(1860)$	$5/2^+$	**	*	**		*	*		
$N(1875)$	$3/2^-$	***	**	**	*	**	*	*	*
$N(1880)$	$1/2^+$	***	**	*	**	*	*	**	**
$N(1895)$	$1/2^-$	****	****	*	*	*	****	**	**
$N(1900)$	$3/2^+$	****	****	**	**	*	*	**	**
$N(1990)$	$7/2^+$	**	**	**			*	*	*
$N(2000)$	$5/2^+$	**	**	*	**	*	*		
$N(2040)$	$3/2^+$	*		*					
$N(2060)$	$5/2^-$	***	***	**	*	*	*	*	*
$N(2100)$	$1/2^+$	***	**	***	**	**	*	*	
$N(2120)$	$3/2^-$	***	***	**	**	**		**	*
$N(2190)$	$7/2^-$	****	****	****	****	**	*	**	*
$N(2220)$	$9/2^+$	****	**	****			*	*	*

Conclusions

- New observed states in the heavy sector are a clear evidence of exotic hadrons
- The hadron spectrum might be full of these kind of states
- New "model independent" tools should be developed to investigate the hadron nature
- The combination of Lattice+EFT might be an interesting technique which can help to elucidate the hadron nature but one should be careful with lattice systematic errors

Thank you